

PCCP

Accepted Manuscript



This is an *Accepted Manuscript*, which has been through the Royal Society of Chemistry peer review process and has been accepted for publication.

Accepted Manuscripts are published online shortly after acceptance, before technical editing, formatting and proof reading. Using this free service, authors can make their results available to the community, in citable form, before we publish the edited article. We will replace this *Accepted Manuscript* with the edited and formatted *Advance Article* as soon as it is available.

You can find more information about *Accepted Manuscripts* in the [Information for Authors](#).

Please note that technical editing may introduce minor changes to the text and/or graphics, which may alter content. The journal's standard [Terms & Conditions](#) and the [Ethical guidelines](#) still apply. In no event shall the Royal Society of Chemistry be held responsible for any errors or omissions in this *Accepted Manuscript* or any consequences arising from the use of any information it contains.

Photoionization of clusters in intense few-cycle near infrared femtosecond pulses

S. R. Krishnan^{*a}, R. Gopal^a, R. Rajeev^b, J. Jha^b, V. Sharma^c, M. Mudrich^d, R. Moshhammer^e and M. Krishnamurthy^{*a,b}

⁵ Received (in XXX, XXX) Xth XXXXXXXXXX 20XX, Accepted Xth XXXXXXXXXX 20XX

DOI: 10.1039/b000000x

In this article we present a perspective on the current state of art in the photoionization of atomic clusters in few-cycle near-infrared laser pulses. Recently, several studies have reported intriguing phenomena associated with the photoionization of clusters by pulses as short as ~10 fs which approach the natural timescales of collective electronic motion in such nanoscale aggregates. In contrast to the dynamics occurring on few- and sub-picosecond timescales where ionic motion sets in and plays a key role marked by resonant plasmon oscillations, the few-cycle limit precludes cluster expansion due to the nuclear motion of ionic constituents. Thus, pulses lasting just a few optical cycles, naturally present a new “impulsive” regime for the first time to explore cluster nanoplasmas in which the ions essentially remain “frozen.” Along with the perspective on this new regime, we present first measurements of photoelectron distributions and temperatures.

¹⁵ Introduction

The investigation of the photoionization of clusters in near-infrared (NIR) fields in the femtosecond domain has been a consequence of breakthroughs and developments in femtosecond laser technology. More recently, the availability of sufficiently intense few-cycle pulses [1] from Ti:Sapphire mode-locked systems has provided opportunities to study photoionization in isolated atoms [2] and molecules [3, 4, 5], and in clusters. While the photoionization of rare-gas and metal clusters in long femtosecond pulses (pulse widths greater than 50 fs) has been studied for over two-decades now and adequately reviewed [6,7], similar investigations with few-cycle pulses are rapidly gaining attention with contemporary and future efforts poised for exciting discoveries. Hence, a perspective on the current state-of-the-art and an outlook towards forthcoming possibilities is timely.

These few-cycle near-infrared pulses, predominantly with a central wavelength of ~800 nm (photon energy ~1.5eV), are said to be “intense” when the peak electric field is comparable to the Coulomb field binding the electron in an atom [8]. Under the influence of such an external electric field, bound electrons can tunnel out through the net potential which is a sum of the native atomic potential and that due to the laser pulse. The laser field acts as a strong time-varying external field which is necessarily non-perturbative [8, 9]. At a central wavelength of 800nm, an optical cycle has a period of ~2.7fs. Thus, pulses with a temporal full-width at half-maximum (FWHM) of 10fs or less may be appropriately described as few-cycle pulses. Such pulses are so short that ionic motion during the interaction of these pulses with the target can be ruled out. Hence, these pulses provide an unprecedented opportunity to investigate clusters in a regime which is entirely dominated by electronic motion in the collective potential of the ions which remain essentially motionless or “frozen” during the interaction with the pulse. In contrast, photoionization dynamics of clusters in the NIR on sub- and few-picosecond timescales is dominated by the motion of ions – the expansion of the ionized aggregate leads to a strong resonant interaction between the driving laser field and the electron-ion system resulting in the so-called nanoplasma resonance.

Generation of clusters – pure and doped

³⁵ Atomic clusters used in photoionization studies are produced by the supersonic expansion of atoms in a gaseous state held at a pre-determined pressure and temperature before expansion through tiny orifice. The dimensions of the orifice and the shape of the outlet together with the thermodynamic parameters determine the size of the atomic clusters which is a log-normal distribution [10, 11]. This is captured using the Hagen parameter:

$$\Gamma = k P_0 \cdot (d / \tan \alpha_{1/2})^{0.85} \cdot T_0^{-2.29}; (1)$$

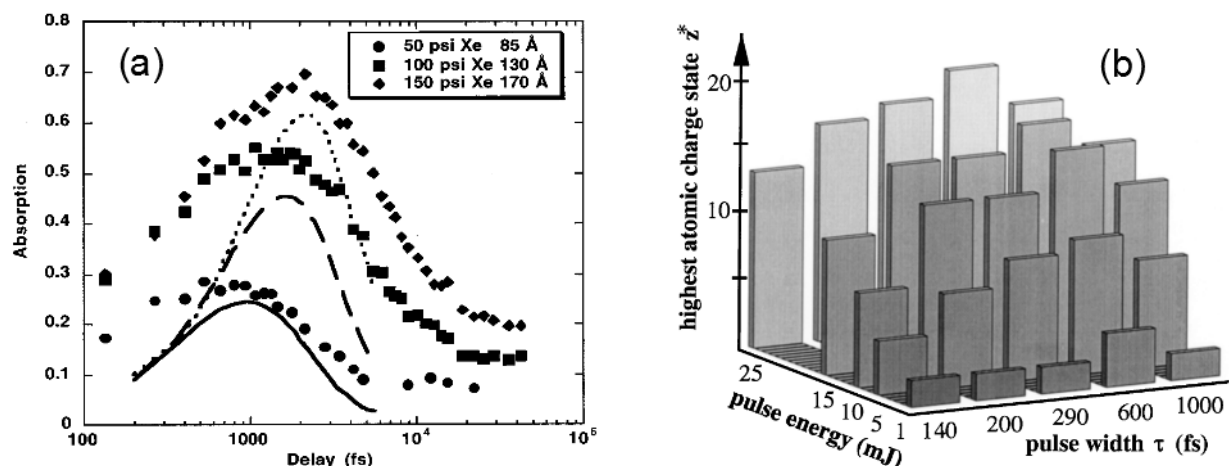


Figure 1 Nanoplasma resonance - absorption and charging observed in experiments: (a) probe absorption as a function of delay between pump and probe pulses for different sizes of Xe clusters as reported in ref. [15] and (b) the maximum charge state measured by Koeller et al. [16] resulting from the photoionization of pure Ag clusters as a function of pulse width for different pulse energies. Both (a) and (b) establish that nanoplasma resonance is a robust phenomenon underlying the ps and sub-ps dynamics. Copyright American Physical Society refs. [15, 16].

where P_0 is the pressure of the gas held at a temperature T_0 before expansion through the nozzle with an orifice diameter d and half-angle of opening $\alpha_{1/2}$. The parameter k depends on the gas being used and determines the propensity of cluster formation. The number of atoms per cluster n is nearly quadratic in T with $n \sim T^q$; the value of q is in the range 1.8 – 2.25 depending on the gas [10, 11, 12]. While this scaling law is commonly used in the case of several rare-gas species, the sizes of helium clusters are often determined by comparing the conditions in use to the calibration curves found in extensive studies performed in the past, summarized by Stienkemeier et al. [13] and Toennies et al. [14]. These jets have been produced in both the continuous [10] as well as pulsed [17] modes of operation.

Doping foreign species into host cluster matrices is done either by passing the jet of these pristine aggregates through a vapour cell containing the dopant atoms or by co-expanding a host-dopant gas mixture. One may also cross a jet of dopant atoms with the beam of host clusters to achieve the same results. For fine control of doping levels the pick-up method is well-suited. In this case, the pick-up of dopants – rare-gases, metals or molecules - from the cell follows Poisson statistics as verified by several experiments [14, 18] and Monte Carlo simulations [19]. These distributions should be taken into account in interpreting experimental results.

Photoionization of clusters in near-infrared fields – the long-pulse case

Nanoplasma resonance

It is appropriate to recapitulate the key aspects of the photoionization dynamics of rare-gas clusters in the long-pulse limit. Studies in this regime have been carried out with pulses 0.1-10ps in duration or equivalently by twin-pulses separated by a variable delay on similar timescales. The most interesting properties of clusters in this domain result from the excellent absorption and coupling of energy from the laser field to the electron-ion system, the nanoplasma, far exceeding what is possible in atomic jets or planar solid targets [6, 7]. This is due to the fact that the dipolar eigenfrequency (Ω) of collective electron oscillations, i.e. plasmons, in the quasi-neutral nanoplasma depends on the charge density ρ and the morphology of the nanoplasma, which for the spherical case is given by [6, 7]:

$$\Omega^2 = 4\pi\rho/3; \quad (2).$$

In typical atomic clusters (1-100nm in diameter), owing to the near-solid density of atoms, the nanoplasma eigenfrequency exceeds the frequency of IR pulses at 800nm as soon as the photoionization process begins [6]. This interaction turns resonant when ionic motion sets in on the timescales of ~ 0.1 -1 ps when the cluster expands lowering the electron density. The decreasing nanoplasma eigenfrequency then matches the frequency of the driving laser field leading to the nanoplasma resonance [6, 15]. This picture of dynamics, also called the nanoplasma model, has been validated by several experiments and ab initio numerical simulations on rare gas and metal clusters (see e. g. refs. [6] and [7]). Both charging of the cluster and absorption of light are enhanced if laser pulse-widths or inter-pulse delay in two-pulse experiments are appropriately chosen to match the timescale of cluster expansion. Figure 1 (after refs. [15, 16]) illustrates the presence of an optimal delay for nanoplasma resonance to occur. Saalman et al. [20] established the occurrence of this resonance phenomenon by showing that the phase difference between motion of the center-of-mass of electrons in the nanoplasma and the driving laser pulse undergoes a $\pi/2$ -flip at the same time as when the damping coefficient, which is a measure of laser pulse absorption, goes over a maximum.

Emission ions, electrons and photons

Several studies spanning a wide-range of laser pulse and intensity parameters have reported the emission of highly-charged ions and energetic electrons resulting from the photoionization of clusters on sub-picosecond and picosecond timescales. In all such cases, the

maximum observed charge-states for ions from the photoionization of clusters far exceeds that observed in isolated atoms – e. g., Snyder et al. [21] observed a maximum charge-state of 20+ for Xe ions resulting from the irradiation of Xe clusters with 350 fs pulses with peak intensities of $\sim 10^{15}$ W/cm², whereas even with intensities as large as 10^{18} W/cm², the highest charge state observed for the case of isolated Xe atoms by Palaniyappan et al. [22] was only Xe¹²⁺ with nonsequential atomic photoionization processes reportedly becoming important. Also, in the case of metal clusters (Pb, Ag, Pt, Au), at peak intensities of 10^{16} W/cm², charge-states as high as 30+ have been

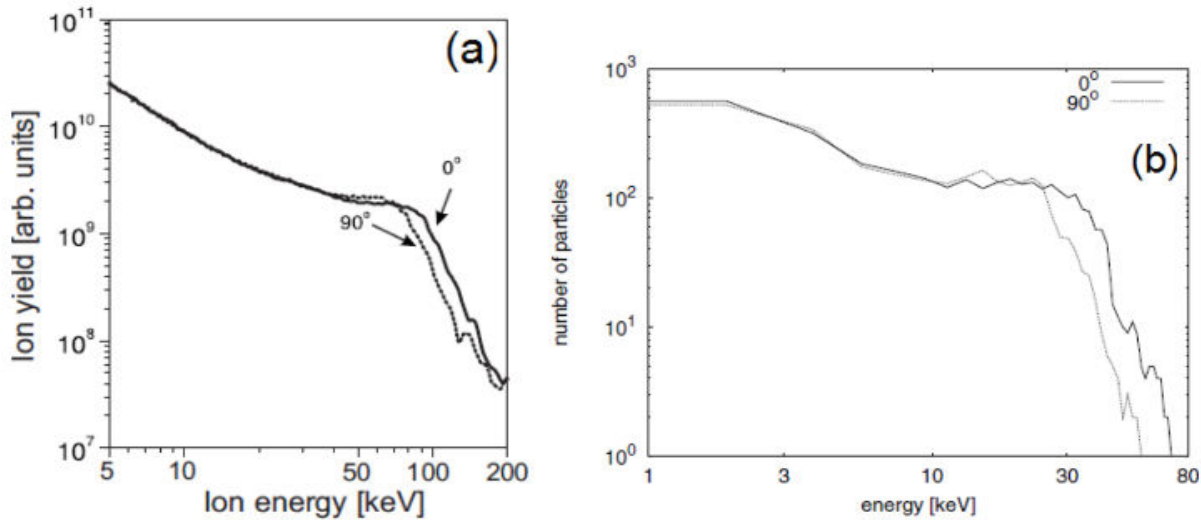


Figure 2 Anisotropic ion emission: (a) experimentally measured ion kinetic energy spectra for Ar₄₀₀₀₀ clusters exposed to 150 fs pulses of a peak intensity 8×10^{15} W/cm² in ref. [27] and (b) result of particle-in-cell simulations by Jungreuthmayer et al. as reported in ref. [28] performed for single clusters using similar parameters as in (a). Copyright American Physical Society, refs. [27, 28]

observed consistently [23, 24] in the long-pulse regime. The observation of higher charge-states in the case of cluster photoionization as compared to isolated atoms clearly indicates the important role of collective effects in the electron-ion dynamics in cluster nanoplasmas. Two key aspects of the dynamics leading to the charging of clusters are – (i) the high local fields in the electron ion system [8] and (ii) the gain in the kinetic energy of quasi-free electrons trapped in the potential of the ions [7]. The net potential of ions (U_{cluster}) in the cluster is largely harmonic [6] for relatively small displacements of the electron cloud from the center of charge of the ions:

$$U_{\text{cluster}}(r, R) = \left\{ \begin{array}{l} -\frac{Q}{2R} \left(3 - \frac{r^2}{R^2} \right), r \leq R ; \\ -\frac{Q}{r}, r \geq R \end{array} \right\}; \quad (3)$$

where r is the radial coordinate, R is the cluster radius and Q is the net ionic charge in the cluster. For large excursions of the electron cloud, this net ionic potential has an anharmonic character [25]. The consequences of electron oscillations in both barrier-lowering for ionization as well as screening within the ionized cluster have been considered in detail by Fennel et al. [26] including a treatment of these effects in ab initio calculations. Further, the local electric field in the cluster due to the relative displacement of the centers of charge of electrons and ions respectively, also called the polarization field, dynamically changes as laser-driven dipolar oscillations of the electron cloud in the ionic cluster potential occurs. This aids further charging of ions by lowering the effective Coulomb barrier and enhancing the rate of tunnel ionization in the cluster as compared to that of an isolated atom (see e.g. Krainov et al. [8]). An immediate consequence of this process is the following: the effect of the polarization field is anisotropic. The ions at the poles of the nanoplasma along the direction of laser polarization (and collective electron oscillation), are charged to a larger extent than those at the equator. Indeed, this was evidenced by Kumarappan et al. [27] who observed that photoions emanating parallel to the direction of laser polarization have kinetic energies larger than those released perpendicular to it. They attributed this to so-called “charge-flipping” which is essentially a consequence of the anisotropic polarization field as the simulations of Jungreuthmayer et al. [28], shown in figure 2, revealed. We will see that this picture does not strictly hold in the case of few-cycle pulse photoionization.

Secondly, quasi-free electrons in the cluster can expend a part of the kinetic energy gained from laser field and ionize the ions further by inelastic collisions (i. e., impact-ionization). The kinetic energy gained by a free electron driven in the laser field of intensity I (W/cm²) and central wavelength λ (μm) is of the order of the ponderomotive energy given (in electron-volts) by $U_p = 9.33 \times 10^{-14} \cdot I \cdot \lambda^2$. In clusters, quasi-electrons can gain kinetic energies as high as $\sim 50U_p$ or more. Lotz cross sections σ_c [29] have been used successfully to estimate the electron-impact ionization even in these dense nanoplasmas:

$$\sigma_c = a_i f_i \frac{\ln(K_e/\Phi_{\text{IP}})}{K_e \cdot \Phi_{\text{IP}}}; \quad (4)$$

were K_e is the electron kinetic energy, Φ_{IP} is the ionization potential for the removal of the next electron from the valence shell containing f_i electrons and a_i is a constant depending on the atomic species. The role and treatment of electron recombination in diminishing ionic charge within the cluster is a developing subject. Peltz et al. [30] have pointed out that the main recombination channel to be considered in these dense nanoplasmas is three-body recombination (TBR) – the capture of an electron by an ion in the vicinity of a second electron. It should be noted here, as pointed out by Krainov et al. [31] and Peltz et al. [30], that due to the local fields in the plasma Rydberg states are not available for recombination. Thus, a cut-off in the maximum principal quantum number should necessarily be employed in estimations of recombination rates. Impact-ionization is also most efficient in under the conditions of resonant energy transfer between the laser field and the driven electron-ion system. Koeller et al. [16] observed that the highest charge-states of photoions, appear at optimal pulse durations (~ 600 fs) which remains constant over a wide range of intensities, corresponding to the

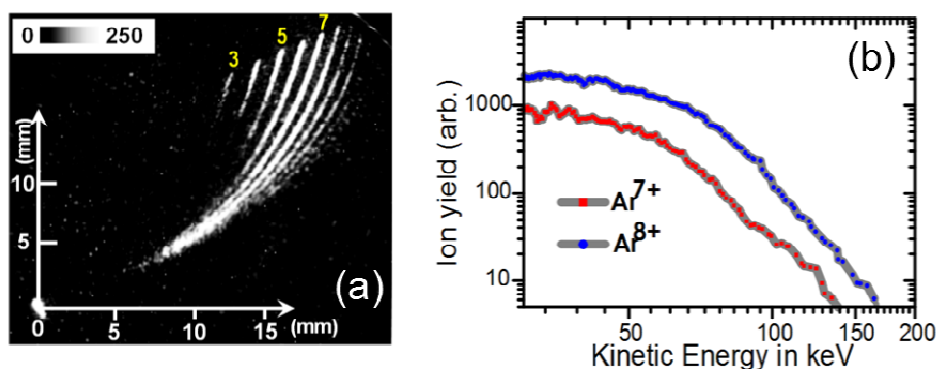


Figure 3 Benchmark two-dimensional charge-state resolved ion kinetic energy distributions: Using a Thomson parabola spectrometer (see ref. [47] for details) kinetic energy distributions of the different charge-states of ions resulting from the photoionization of Ar clusters by 150fs pulses ($\sim 10^{16}$ W/cm²) can be obtained. (a) The “parabolas” seen as is on the imaging microchannel plate detector are shown. Along each parabola, the mass/charge of the impinging ion remains constant while the kinetic energy varies. The charge-states increase from left to right and the three representative charge-states of positively Ar ions, 3, 5 and 7 are marked. (b) The kinetic energy distributions of Ar⁷⁺ and Ar⁸⁺ ions obtained from the corresponding parabolas in (a) are presented, for details of the procedure see ref. [47].

10 occurrence of a nanoplasma resonance.

As expected from the preceding discussion on photoion emission, photoelectrons too may be expected to carry signatures of the strong anisotropic local polarization fields operating in the nanoplasma. Owing to collective oscillations and resonance in the nanoplasma, photoelectrons emitted from clusters have kinetic energy distributions with tails extending to more than $50U_p$ [7, 32], whereas in the case of isolated atoms classical theory sets a limit of about $10U_p$ [33]. In the case of Xe clusters, the ratio of the fast electron yield parallel to the laser polarization (Y_{\parallel}) to that of the perpendicular component (Y_{\perp}) was measured to be about 3.5 [34], while another study on Ag clusters demonstrated a Y_{\parallel}/Y_{\perp} ratio greater than 6 [32]. It should be mentioned that a direct comparison of these ratios between different experiments is difficult since the Y_{\parallel}/Y_{\perp} depends on the solid-angle of collection of photoelectrons which is not necessarily the same in all studies. In the study on Ag clusters [32], a comparison of experiments to ab initio calculations revealed a dominant mechanism for electron acceleration: quasi-free electrons which maintain an appropriate phase relationship with the plasmon oscillations synchronized with the laser field benefit from timely recollisions with the ionic core after excursions away from the center. This acceleration which occurs predominantly in the surface region of the ionic core due to the local polarization field in the nanoplasma, has been appropriately termed as surface plasmon-assisted recollision (SPARC). Since the polarization field is maximal when nanoplasma resonance is achieved, the Y_{\parallel}/Y_{\perp} ratio follows this trend [32]. Extending the phenomenon first observed in atoms, Saalman et al. [35] provided an elegant generalization of the momentum gained by electrons following their recollision with an extended potential well. In latter case, the momentum gain depends not only on the vector potential of the driving laser field but also on the length of the attractive potential of extended systems such as clusters.

An important consequence of the presence of highly-charged ions and energetic is photo-emission from bound-bound transitions and recombination in these nanoplasmas, particularly in the inner atomic shells. Characteristic x-ray emission (e.g. K_{α} -x-rays) from a variety of clusters has been measured [36, 37, 38]. In the long-pulse regime, once again, short wavelength emission from inner-shell transitions was found to maximize at the optimal pulse-length (or -delay) corroborating nanoplasma resonance. Indeed, doping Ar clusters with ($\sim 1\%$) H₂O [37] led to an enhancement of the yield in Ar characteristic x-rays over pure Ar clusters. A similar enhancement in the maximal charge-state of Ar ions from HI doped Ar clusters has also been observed [40].

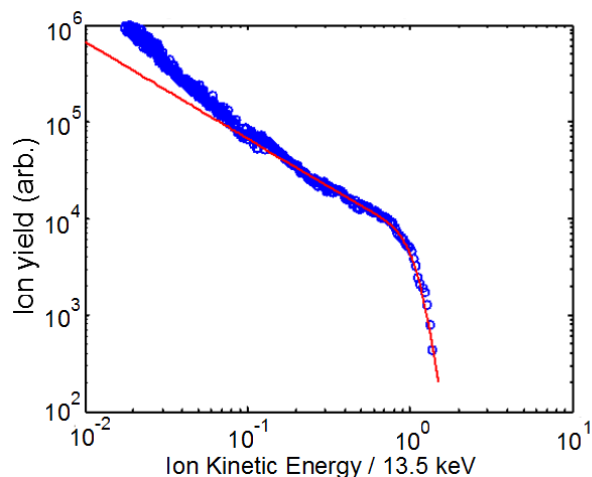


Figure 4 Ion kinetic energy distribution from Ar clusters photoionized by 7fs pulses with a peak intensity of 2×10^{15} W/cm². The data (blue circles) is best-fit (red line) with the scheme of Islam et al. [42].

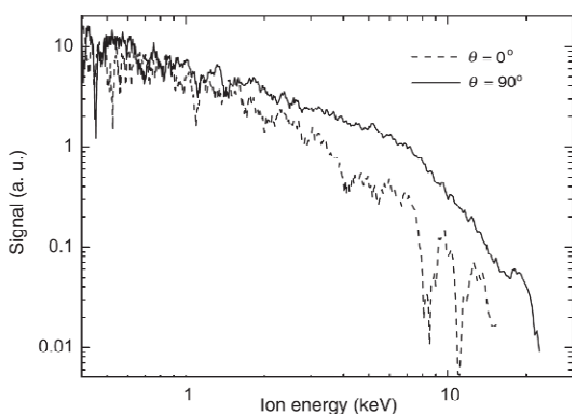


Figure 5 Anomalous anisotropy in the kinetic energy distribution of ions in the few-cycle regime as reported by Skopalova et al. [50]. The ions emerging parallel to the direction of laser polarization (0° , dotted curve) and those emanating perpendicular to it (90° , solid curve) are shown. This picture is in contrast to the observation made in the long-pulse regime presented (see figure 2), as discussed in the text. Copyright American Physical Society, ref. [50].

In the long-pulse limit, cluster disintegration on ps timescales also has led to several interesting consequences and has been used as a probe for effects of the dynamics during the interaction with the laser pulse. The expansion of the ionic core of the cluster which is crucial for attaining nanoplasma resonance, also leads to a lowering of the height of the cluster potential that withhold quasi-free electrons from leaving the cluster. When this is no longer the case, electrons boil-off the cluster potential leaving behind a net positive charge. Both the pressure on ions due to mutual Coulombic repulsion as well as the (attractive) pressure of the expanding electron gas on ions act to dismantle the ionic core leading to high-energy photoion emission [6, 7]. The resultant high kinetic energy of ions was exploited to demonstrate nuclear fusion in deuterium clusters [41]. Islam et al. [42] showed that the characteristic shape of ion kinetic energy spectra (figure 2) can be deduced by a combination of the Coulomb explosion profile of uniformly charged clusters with averaging over laser intensities in the focal volume, the distribution of cluster sizes and including possible saturation in the charging process. Subsequently, Peano et al. [43] showed that (at intensities $\sim 10^{16}$ W/cm²) the shape of the ion kinetic energy distributions depend on the ratio of the Coulombic potential energy and the thermal energy of the electron gas, thus calling for a more careful application of the purely Coulombic picture. In cases where the cluster is stripped of most electrons at an early stage, ion kinetic energy distributions can carry signatures of phenomena such as formation of shock shells [44], ion overtake [45] and indeed even alignment in molecular clusters [46]. As a result deriving information about the dynamics ensuing during the interaction with the laser pulses from such ion kinetic energy distributions (without resolving their charge-states) is not straightforward. A recent development in this regard is the demonstration of obtaining two-dimensional kinetic energy distributions of ions by the group lead by one of the authors [47, 48] – the kinetic energy distributions of each individual ionic charge-state can be obtained using Thomson parabola spectrometers. A benchmark two-dimensional spectrum and the kinetic energy distributions are presented in figure 3. The use of this spectrometer in combination with time-of-flight analysis lead to the discovery that high-energy neutral atoms as well as fast negative ions from molecular clusters can be generated using cluster nanoplasmas [48].

Intense near-IR few-cycle pulses and photoionization of clusters

It is clear from the preceding discussions that cluster expansion and ionic motion are necessary for nanoplasma resonance to occur on ps and sub-ps timescales. This mechanism is essentially turned-off by employing few-cycle pulses (~ 10 fs) since the motion of ions can be neglected on these timescales [6, 7]. Consequently, few-cycle pulses act as an “impulse” with regard to ionic motion. By excluding the key operational mechanism in the long-pulse case, few-cycle pulses open up a new regime for exploration. The remainder of this article is devoted to the new science emerging on these timescales.

Generation and use of intense few-cycle pulses

Amplified few-cycle pulses in at NIR wavelengths with durations as short as 10fs are produced using mode-locked Ti:Sapphire based laser systems. Following conventional chirped-pulse amplification, spectral broadening using a gas-filled hollow fiber and subsequent recompression by chirped-dielectric mirrors produce few-cycle pulses with typical energies as high as a few mJ at repetition rates higher than 1kHz [1]. The width of these pulses is measured using well-established techniques such as coherent autocorrelation, frequency-resolved optical gating and spectral interferometry [49]. Typically, these pulses are focussed onto a cluster jet in a vacuum chamber and photo-fragments are subsequently measured using a suitable spectrometer [52].

Photoion emission – a counter-intuitive picture

We measured the photoion kinetic energy spectrum from Ar clusters subject to 7fs pulses with an intensity of 2×10^{15} W/cm² which is presented in figure 4. Clearly the ion kinetic energy (KE) distribution is very similar to observations the long-pulse regime (figure 2). Although the physics of ion emission in this “frozen” regime seems similar to the long-pulse case, a comparison of ion KE distributions parallel and perpendicular, relative to the laser polarization direction reveals a surprising counter-intuitive phenomenon. Unlike in the long-pulse case, the maximum KE of ions in the direction perpendicular to the laser polarization (E_{\perp}) is greater than that of the ions emerging in the parallel (E_{\parallel}) direction, $E_{\perp} > E_{\parallel}$, as reported by Skopalova et al. [50] and is evident in figure 5. The picture of a strong polarization force within the cluster leading to higher charging at the poles in the long-pulse regime [27] leading to $E_{\parallel} > E_{\perp}$ does not hold for in the case of few-cycle pulses. Indeed, Skopalova et al. [50] recovered the latter case ($E_{\parallel} > E_{\perp}$) by stretching the pulses to durations longer than 150fs, when ionic motion in these systems sets in. They reasoned the counter-intuitive behaviour in the impulse regime ($E_{\perp} > E_{\parallel}$) using the motion of a uniform quasi-free electron cloud with a size smaller than the cluster ionic core. As a consequence of their limited extent within the cluster, the electron cloud repeatedly screens the poles during the driven oscillations but leaves the equatorial region unscreened. Thus, greater charge develops along the equator leading to the observed anomalous anisotropy [50, 51]. Although a qualitative picture has emerged to account for the atypical anisotropy observed in the impulsive regime, the role of screening and recombination which is well-understood in the long-pulse regime [30, 52], needs to be investigated in detail for the case of few-cycle pulses. Sub-cycle dynamics leading to breaking of the plasma waves in the cluster and the consequent formation “hot-spots” on few-femtosecond timescales examined by Varin et al. [53] could also play a significant role in the interaction with such short pulses.

Designing nanoplasmas for resonances in few-cycle pulses and dopant-induced ignition

It is clear from the discussions in the preceding sections dedicated to the long-pulse limit that ionic motion on sub-ps timescales is a necessary pre-requisite to bring the over-dense cluster nanoplasma to sufficient dilution whereby a resonance between the collective electron oscillations and the driving laser field can occur. Thus, on timescales of 10fs or less, when the ionic core remains frozen, conventional nanoplasma resonance due to cluster expansion cannot occur. Mikarberidze et al. [54] pointed out a mechanism for the resonant coupling of laser pulses which can occur due to nanoplasma morphology, without the need for ionic motion or the consequent lowering of plasma density within the cluster. They proposed ionizing doped He nanodroplet (with the dopant Xe atoms residing at the center) using laser pulses which have a carefully chosen intensity such that only the dopants, but not the He, atoms are directly ionized by the optical field. Beginning with the “seed” electrons released from the Xe atoms, the ionization of He occurs as the linearly polarized laser field drives them along the direction of its oscillating electric field. Consequently, the ionization of the doped droplet proceeds inside-out and a nanoplasma is created inside the neutral host medium as the laser pulse ramps in intensity. Remarkably, the resonant

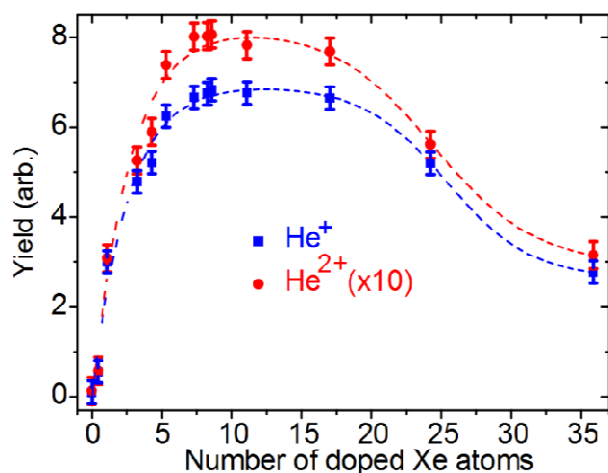


Figure 6 Dopant-induced ignition: The yield of He⁺ and He²⁺ ions from Xe doped He nanodroplets as a function of the number of doped atoms, after ref. [55]. The charging of the nanoplasma in droplets containing 10^4 He atoms saturates for a doping number of just 7. The fall in yield at large doping numbers (>20 doped Xe atoms) is to droplet beam destruction Copyright American Physical Society, ref. [55].

coupling of the laser field with this ellipsoidal nanoplasma leads to the complete ionization of all the 10^4 host atoms in the He nanodroplet even with a very weak doping of less than 10 Xe atoms. The experiments by Krishnan et al. [55] confirm this: under intense 10fs pulse irradiation, the yield of He⁺ and He²⁺ ions as a function of the number of doped Xe atoms in the He nanodroplets (containing 15000 He atoms on average) was found to increase sharply and saturate for a doping number of just 7 leading to dopant-induced ignition, as shown in figure 6.

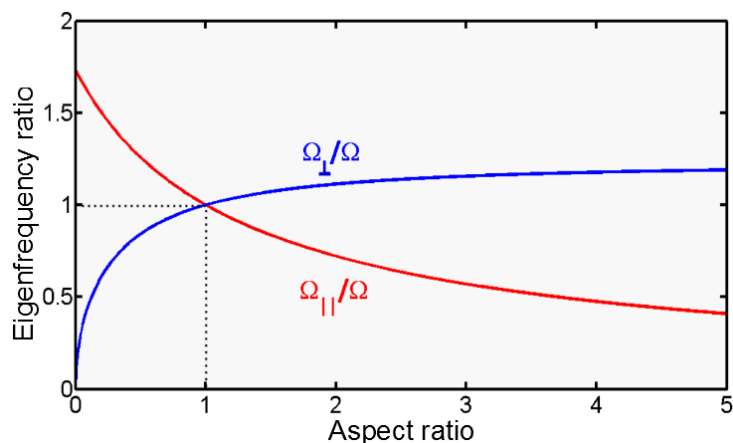


Figure 7 Eigenfrequencies of the ellipsoidal nanoplasma along the major and minor axes as a function of the ellipsoid aspect ratio, scaled by the eigenfrequency for a spherical plasma with identical charge density [see also refs. 54, 56, 57].

The main reason underlying this dramatic turnaround from transparent pure He nanodroplets to active doped clusters is the onset of a new nanoplasma resonance mechanism occurring on timescales less than 10fs. Similar to the long-pulse case, understanding the interaction between few-cycle pulses and these doped droplets requires an examination of the interrelation between the laser frequency (ω) and the eigenfrequencies of the embedded nanoplasma. Since this nanoplasma is formed by the collective driving of electrons along the direction of laser polarization, the morphology of the electron-ion system is ellipsoidal, or cigar-shaped [54]. The ellipsoidal ionic potential in which the quasi-free electrons oscillate has two characteristic frequencies – the first is the eigenfrequency for oscillations along the major axis of the ellipse parallel to the laser polarization vector Ω_{\parallel} , while the other mode orthogonal to the driving electric field has a natural frequency Ω_{\perp} . These eigenfrequencies depend on the charge density ρ and the aspect ratio α of the ellipsoid. Using the eigenfrequency (Ω) of a spherical nanoplasma with an identical charge density ρ , (see equation 1), Ω_{\parallel} and Ω_{\perp} may be written as [56, 57]:

$$\Omega_{\parallel} = \Omega \cdot g(\alpha) \text{ and } \Omega_{\perp} = \Omega \cdot h(\alpha); \quad (5)$$

where, $g(\alpha)$ and $h(\alpha)$ are decreasing and increasing functions of α , respectively. The detailed expressions for $g(\alpha)$ and $h(\alpha)$ plotted in figure 7 can be found in refs. [56, 57]. Since the aspect ratio of the nanoplasma increases with the growth of charge within the nanodroplet, the relevant eigenfrequency component Ω_{\parallel} drops and matches the driving frequency of the laser (ω):

$$\Omega_{\parallel} = \omega; \quad (6).$$

Fortuitously, this condition is achieved close to the intensity peak of the pulse [54], whereupon resonant driving of electrons leads to the complete ionization of the host He atoms.

Photoelectron emission

The emission of photoelectrons from cluster nanoplasmas in intense few-cycle pulse interactions is an aspect of the dynamics complementary to photoion generation. El-Taha et al. [58] measured photoelectron emission from Xe clusters with a time-delayed pair of ~ 11 fs pulses and intensity fractions of 0.3 and 0.7 for the first (leading) and second (probe) pulses respectively. The measured electron yields showed a characteristic pump-probe dependence on a ps-timescale. The maximum yield of electrons was found to occur at an optimal delay which depended on the size of the cluster. It should be mentioned that although this two-pulse study employs few-cycle

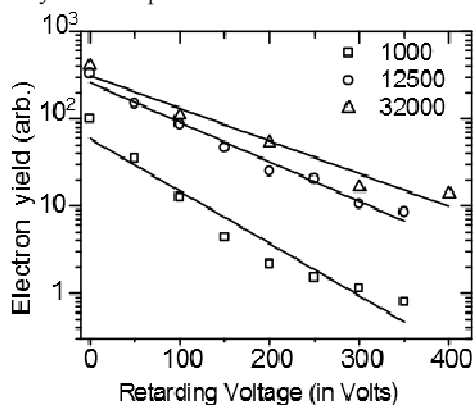


Figure 8 Retarding potential analysis of photoelectrons emitted by Ar clusters of different sizes (in the legend) ionized by 7fs pulses ($\sim 10^{15}$ W/cm²). The temperatures of the distributions are 46eV, 81eV and 107eV for clusters containing 1000 (\square), 12500 (\circ) and 32000 (Δ) Ar atoms per clusters, respectively. Lines to guide the eye.

pulses, the phenomenology investigated clearly belongs to the long-pulse regime.

We present here for the first-time, to the best of our knowledge, photoelectron emission measurements in the few-cycle limit. Our experimental set-up is similar those employed in several previous investigations [59]. In our experiment, Ar clusters (sizes in the range 1000 – 32000) were ionized by 7fs pulses ($\sim 10^{15}$ W/cm²). The time-of-flight signals from photoelectrons impinging a microchannel plate detector was recorded. In order to obtain signals specific to photoelectrons and differentiate these from photons which could simultaneously arrive at the detector due to delayed photoemissions, we employed a retarding electric field ahead of the detector which allowed us to selectively collect only those photoelectrons which have a kinetic energy sufficient to overcome this applied potential barrier. Indeed applying retarding potentials is important as the studies of Springate et al. [60] and Kumarappan et al. [34] revealed.

Figure 8 shows the relative electron yield as a function of the retarding voltage applied for 3 different sizes of Ar clusters - 1000, 12500 and 32000 atoms per cluster. From these integrated electron yields as function of retarding voltage, we obtain the photoelectron temperatures following Jha et al. [59]. Noting that the photoelectrons emitted have an exponential distribution of kinetic energies, we may write the corresponding energy distribution function:

$$s(E) = s_0 e^{-E/kT}; \quad (7)$$

where k is the Boltzmann constant, T the temperature of the distribution, E is the photoelectron kinetic energy and s_0 is a constant. Since the application of a retarding potential V results in the detector collecting photoelectrons with kinetic energies $E > V$, the yield of electrons measured by the detector as a function of the retarding potential $S(V)$ is:

$$S(V) = \int_{E>V}^{\infty} dE s_0 e^{-E/kT} = s_0^2 kT e^{-V/kT}; \quad (8)$$

It is clear from equation 8 that the temperature of the photoelectron kinetic energy distribution can be obtained from $S(V)$. Employing this method which was also used by Jha et al. [59], we determined that the temperature of the photoelectrons from these Ar nanoplasmas increases from 46 eV to 107 eV as the size of the cluster is increased from 1000 to 32000 atoms per aggregate. The temperatures measured here are in the range of values obtained earlier [59] with 150fs pulses ($\sim 10^{15}$ W/cm²) in the nonimpulsive regime. However, it is clear from the work of Skopalova et al. [50] on Ar (and Xe) clusters that the key aspects such as the extent of the electron cloud within the cluster are fundamentally different in the impulsive regime as compared to the long-pulse case. Thus, acceleration mechanisms from which electrons gain their kinetic energy are significantly different in the few-cycle limit. Clearly, further theoretical and numerical investigations are required to uncover the underlying physics.

Carrier envelope phase effects

Since the carrier wave has an optical cycle of ~ 3 fs for pulses with a central wavelength of ~ 800 nm, in pulses with a temporal full-width at half-maximum of 5s or less, the shape of the electric field within the becomes an important factor. This unique feature of few-cycle pulses can be quantified by the relative phase between the maxima of the pulse envelope and that of the electric field of the carrier wave, or carrier-envelope phase (CEP), which is a measurable quantity [61]. Single-shot CEP measurements have been demonstrated and used to perform experiments on atomic systems [61]. In the case of atoms and molecules, several studies have demonstrated that electron dynamics depends upon and can even be controlled using the CEP of such pulses (see e.g., refs. [2 - 5]).

There are very few studies of CEP effects on the photoionization of nanoscale media. Zherebstov et al. [62] reported an impressive study of the photoionization of silica (SiO₂) nanoparticles with diameters of 50-150nm using 5fs pulses with intensities in the range $1-5 \times 10^{13}$ W/cm². In this case a direct comparison of photoelectron emission between Xe atoms and silica nanospheres informs us about the key role played by CEP in the steering of photoelectrons released from extended targets. In terms of the ponderomotive energy defined earlier, the photoelectrons from Xe atoms carried away a kinetic energy with a cut-off of close to $10U_p$. For the nanoparticles the observed cut-off in the photoelectron kinetic energy extended beyond $50U_p$. In both cases, the photoelectrons were sensitive to CEP and were emitted anisotropically with faster electrons emanating along the direction of laser polarization. For the nanoparticles, at an intensity of 1.9×10^{13} W/cm², corresponding to a U_p of 1.2eV, the asymmetry of photoelectron emission, characteristic of CEP effects was observed for kinetic energies above 10eV all the way to 47eV. An immediate conclusion from the CEP dependence is that the electron acceleration mechanisms dominant in extended systems depend on the instantaneous electric field of the laser and sub-cycle phenomena therein are important. This also paves way to control and manipulate these processes by manoeuvring the shape of electric field within the pulse.

Although this experiment demonstrates CEP sensitivity, it should be pointed out that the peak intensities used in this study are considerably lower than those used in studies on atomic clusters discussed in earlier sections. Here, the Keldysh adiabaticity parameter γ has values in the range 1.0 -1.5, for both Xe and silica thus falling in the intermediate region between multiphoton ($\gamma > 1$) and tunnelling ($\gamma < 1$) regimes for atoms [9]. The experiments discussed earlier were clearly in the $\gamma < 1$ limit and were being performed on relatively smaller clusters, with diameters less than 100nm (mostly ~ 10 -50nm). For this reason the CEP dependent mechanisms responsible for electron acceleration in this case cannot be generalized to other scenarios discussed earlier. However, this investigation highlights the key role played by CEP dependent phenomena in extended atomic systems and motivates the need for further experiments with CEP control at higher laser pulse intensities. In this context, the simulations of Varin et al. [53] provide insights on the sub-cycle dynamics at higher laser intensities than those considered in the silica nanosphere case.

In this context, a report by Köhn and Fennel in this journal [63] suggested spectral interferometry as a means of extracting information about the dynamics occurring in sub-cycle timescales based on a theoretical microscopic analysis: characteristics of collective electron motion, namely the period and lifetime of plasmon oscillation along with the phase and relative amplitude, can possibly be extracted with sub-cycle resolution, while the experimental realization of this scheme remains to be seen. Similarly, Kundu et al. [64, 65] suggested using harmonic emission from clusters as a probe for possible nonlinear resonances occurring in the collective electron motion in clusters within a few optical cycles due to the anharmonicity of the ionic potential in pristine clusters. Successful observation of these optical emissions requires significantly large number densities of clusters ($> 10^8$ per cm³) as can be obtained near the exit of nozzles used for producing clusters as well as developing schemes to distinguish these coherent emissions from that due to recombination or atomic transitions.

Conclusions and outlook

Intense few-cycle near-IR pulses have opened up a plethora of intriguing phenomena and physics to be investigated in the near future. In comparison with the long-pulse regime, counter-intuitive observations like the anomalous anisotropy in ion emission as well as the need to understand effects carried over from the long-pulse case into the impulse regime such as the acceleration of electrons to kinetic energies of the order of $\sim 500\text{eV}$ within 10fs require a combination of experiments and theory to lead to a better understanding. A natural extension of these studies with few-femtosecond pulses is using isolated as well as trains of attosecond pulses as probes for the collective dynamics. Indeed photoemission in solids investigated with attosecond pulses [66] and observation of phenomena such as metallization of insulators [67] on sub-fs timescales are areas open for research. Finally, using few-cycle IR pulses in combination with extreme-ultraviolet pulses from table-top sources as well as soft- and hard-xray pulses from free-electron lasers [68] are prospects for the future and are forthcoming perspectives.

Notes and references

^a Tata Institute of Fundamental Research (Hyderabad), Hyderabad 50075, India. Tel: +91 9440 264 291, Email: srk@tifrh.res.in

^b Tata Institute of Fundamental Research, 1 Homi Bhabha road, Mumbai 400001, India . Tel: +91 22 2278 2685 ; E-mail: mkrism@tifrh.res.in

^c Indian Institute of Technology – Hyderabad, Yeddumailaram, Hyderabad 502205, India

^d Physikalisches Institut, Universität Freiburg, Hermann-Herder-Str. 3, 79104 Freiburg, Germany.

^e Max-Planck-Institut für Kernphysik, Saupferchekweg 1, D-69117 Heidelberg, Germany.

1. T. Brabec and F. Krausz, Rev. Mod. Phys. 2000, **72**, 545.
2. R. Gopal, K. Simeonidis, R. Moshhammer, Th. Ergler, M. Dürr, M. Kurka, K.-U. Kühnel, S. Tschuch, C.-D. Schröter, D. Bauer, and J. Ullrich, Phys. Rev. Lett. 2009, **103**, 053001.
3. M. F. Kling, Ch. Siedschlag, A. J. Verhoef, J. I. Khan, M. Schultze, Th. Uphues, Y. Ni, M. Uiberacker, M. Drescher, F. Krausz, M. J. J. Vrakking, Science 2006, **312**, 246.
4. Kremer, B. Fischer, B. Feuerstein, V. L. B. de Jesus, V. Sharma, C. Hofrichter, A. Rudenko, U. Thumm, C. D. Schröter, R. Moshhammer, and J. Ullrich, Phys. Rev. Lett. 2009, **103**, 213003.
5. B. Fischer, M. Kremer, T. Pfeifer, B. Feuerstein, V. Sharma, U. Thumm, C. D. Schröter, R. Moshhammer, and J. Ullrich, Phys. Rev. Lett. 2010, **105**, 223001.
6. U. Saalman, Ch. Siedschlag and J. –M. Rost, J. Phys. B 2006, **39**, R39.
7. Th. Fennel, K.-H. Meiwes-Broer, J. Tiggesbäumker, P.-G. Reinhard, P. M. Dinh and E. Suraud Rev. Mod. Phys. 2010, **82**, 1793.
8. V. Krainov, M. B. Smirnov, Phys. Rep. 2002, **370**, 137.
9. M. Protopapas, C. H. Keitel, P. L. Knight, Rep. Prog. Phys. 1997, **60** 389.
10. O. F. Hagena and W. Obert, J. Chem. Phys. 1972, **56**, 1793.
11. R. A. Smith, T. Ditmire, J. W. G. Tisch, Review of Scientific Instruments 1998, **69**, 3798.
12. F. Dorchies, F. Blasco, T. Caillaud, J. Stevefelt, C. Stenz, A. S. Boldarev, and V. A. Gasilov, Phys. Rev. A 2003, **68**, 023201.
13. F. Stienkemeier, K. Lehmann, J. Phys. B: At. Mol. Opt. Phys. 2006, **39**, R127.
14. J. P. Toennies, A. F. Vilesov Angw. Chem. 2004, **43**, 2622.
15. J. Zweiback, T. Ditmire, and M. D. Perry, Phys. Rev. A 1999, **59**, 3166.
16. L. Köller, M. Schumacher, J. Köhn, S. Teuber, J. Tiggesbäumker, and K. H. Meiwes-Broer, Phys. Rev. Lett. **82**, 3783–3786 (1999).
17. U. Even, J. Jortner, D. Noy, N. Lavie and C. Cossart-Magos, J. Chem. Phys. 2000, **112**, 8068.
18. J. Tiggesbäumker and F. Stienkemeier, Phys. Chem. Chem. Phys. 2007, **9**, 4748.
19. O. Bünermann and F. Stienkemeier, Eur. Phys. J. D 2011, **61**, 645.
20. U. Saalman and J. –M. Rost, Phys. Rev. Lett. 2003. **91**, 223401.
21. E. M. Snyder, S. A. Buzza, and A. W. Castleman, Jr, Physical Review Letters 1996, **77** 3347.
22. S. Palaniyappan, A. DiChiara, I. Ghebregziabher, EL Huskins, A. Falkowski, D. Pajeroski, and B. C. Walker, Journal of Physics B 2006, **39** S357.
23. M. A. Lebeault, J. Viallon, J. Chevalyere, C. Ellert, D. Normand, M. Schmidt, O. Sublemontier, C. Guet, and B. Huber, European Physical Journal D **20** (2002), no. 2, 233–242.
24. M. Schumacher, S. Teuber, L. Köller, J. Köhn, J. Tiggesbäumker, and K. H. Meiwes-Broer, European Physical Journal D **9** (1999), 411.
25. M. Kundu and D. Bauer, Phys. Rev. Lett. 2006, **96**, 123401.
26. Th. Fennel, L. Ramunno, T. Brabec, Phys. Rev. Lett. 2007, **99**, 233401.
27. V. Kumarappan, M. Krishnamurthy, and D. Mathur, Phys. Rev. Lett. 2001, **87**, 085005.
28. Jungreuthmayer, M. Geissler, J. Zanghellini, T. Brabec, Phys. Rev. Lett. 2004, **92**, 133401.
29. W. Lotz, Z. Phys. A 1968, **241**, 216.
30. Ch. Peltz and T. Fennel, Euro. Phys. J. D 2011, **63**, 281.
31. V. P. Krainov, A. V. Sofronov, Contributions to Plasma Physics 2007, **47**, 234.
32. T. Fennel, T. Döppner, J. Passig, C. Schaal, J. Tiggesbäumker, and K.H. Meiwes-Broer, Phys. Rev. Lett. 2007, **98**, 143401.
33. G. G. Paulus, W. Becker, W. Nicklich, and H. Walther, J. Phys. B 1994, **27**, L703.
34. V. Kumarappan, M. Krishnamurthy, and D. Mathur, Phys. Rev. A 2003, **67**, 043204.
35. U. Saalman and J. –M. Rost, Phys. Rev. Lett. 2008, **100**, 133006.
36. V. Kumarappan, M. Krishnamurthy, D. Mathur, and L. C. Tribedi, Phys. Rev. A 2001, **63**, 023203.
37. J. Jha, D. Mathur, M. Krishnamurthy, J. Phys. B 2005, **38**, L291.
38. C. Deiss, N. Rohringer, J. Burgdörfer, E. Lamour, C. Prigent, J. –P. Rozet, and D. Vernhet, Phys. Rev. Lett. 2006, **96**, 013203.
39. J. Jha and M. Krishnamurthy, Appl. Phys. Lett. 2008, **92**, 191108.

-
40. J. Purnell, E. M. Snyder, S. Wei, A. W. Castleman Jr., *Chem. Phys. Lett.* 1994, **229**, 333.
41. T. Ditmire, J. Zweiback, V. P. Yanovsky, T. E. Cowan, G. Hays and K. B. Wharton, *Nature* 1999, **398**, 489.
42. Md. Ranaul Islam, Ulf Saalman, and Jan M. Rost, *Phys. Rev. A* 2006, **73**, 041201(R).
43. F. Peano, F. Peinetti, R. Mulas, G. Coppa, and L. O. Silva, *Phys. Rev. Lett.* 2006, **96**, 175002.
44. M. Grech, R. Nuter, A. Mikaberidze, P. Di Cintio, L. Gremillet, E. Lefebvre, U. Saalman, J. M. Rost, and S. Skupin, *Phys. Rev. E* 2011, **84**, 056404.
45. M. Hohenberger, D. R. Symes, K. W. Madison, A. Sumeruk, G. Dyer, A. Edens, W. Grigsby, G. Hays, M. Teichmann, and T. Ditmire, *Phys. Rev. Lett.* 2005, **95**, 195003.
46. Ulf Saalman, Alexey Mikaberidze, and Jan M. Rost, *Phys. Rev. Lett.* 2013, **110**, 133401.
47. R. Rajeev, K. P. M. Rishad, T. Madhu Trivikram, V. Narayanan and M. Krishnamurthy, *Rev. Sci. Inst.* 2011, **82**, 083303.
48. R. Rajeev, T. Madhu Trivikram, K. P. M. Rishad, V. Narayanan, E. Krishnakumar and M. Krishnamurthy, *Nature Physics* 2013, **9**, 185.
49. F.X. Kärtner (Ed.) *Few-Cycle Laser Pulse Generation and Its Applications*. Vol. 95. Springer, 2004.
50. E. Skopalová, Y. C. El-Taha, A. Zaïr, M. Hohenberger, E. Springate, J. W. G. Tisch, R. A. Smith, and J. P. Marangos, *Phys. Rev. Lett.* 2010, **104**, 203401.
51. G. Mishra and N. K. Gupta, *Euro. Phys. Lett.* **2011**, **96**, 63001.
52. S R Krishnan, Ch Peltz, L Fechner, V Sharma, M Kremer, B Fischer, N Camus, T Pfeifer, J Jha, M Krishnamurthy, C-D Schröter, J Ullrich, F Stienkemeier, R Moshhammer, Th Fennel and M Mudrich, *New J. Phys.* 2012, **14**, 075016.
53. C. Varin, C. Peltz, T. Brabec, and T. Fennel, *Phys. Rev. Lett.* 2012, **108**, 175007.
54. A. Mikaberidze, U. Saalman, and J. M. Rost, *Phys. Rev. Lett.* 2009, **102**, 128102.
55. S. R. Krishnan, L. Fechner, M. Kremer, V. Sharma, B. Fischer, N. Camus, J. Jha, M. Krishnamurthy, T. Pfeifer, R. Moshhammer, J. Ullrich, F. Stienkemeier, M. Mudrich, A. Mikaberidze, U. Saalman and J. -M. Rost, *Phys. Rev. Lett.* 2011, **107**, 173402.
56. S. R. Krishnan, Ph. D. Thesis, University of Heidelberg (2011) and A. Mikaberidze, Ph. D. Thesis, Technical University, Dresden (2012).
57. L.D. Landau and E.M. Lifschitz, *Course of theoretical physics: The classical theory of fields*, Vol. 2, Pergamon Press., 2009.
58. Y. C. El-Taha, E. Springate, R. Carley, F. Rajgara, D. Darios, C. Froud, S. Bonora, D. Symes, J. W. G. Tisch, R. A. Smith, D. Mathur, J. P. Marangos, *Lasers and Electro-Optics*, ISBN 978-1-55752-859-9, 2008.
59. J. Jha and M. Krishnamurthy, *J. Phys. B* 2008, **41**, 041002.
60. E. Springate, S. A. Aseyev, S. Zamith, and M. J. J. Vrakking, *Phys. Rev. A* 2003, **68**, 053201.
61. T. Wittmann, B. Horvath, W. Helml, M. G. Schätzel, X. Gu, A. L. Cavalieri, G. G. Paulus and R. Kienberger, *Absolute-phase phenomena in photoionization with few-cycle laser pulses*. *Nature* 2001, **414**, 182.
62. S. Zherebtsov, T. Fennel, J. Plenge, E. Antonsson, I. Znakovskaya, A. Wirth, O. Herrweth, F. Süßmann, Ch. Peltz, I. Ahmad, S. A. Trushin, V. Pervak, S. Karsch, M. J. J. Vrakking, B. Langer, C. Graf, M. I. Stockman, F. Krausz, E. Rühl, M. F. Kling, *Nat. Phys.* 2011, **7**, 656.
63. J. Köhn and T. Fennel *Phys. Chem. Chem. Phys.* 2011, **13**, 8747.
64. M. Kundu, S. V. Popruzhenko, D. Bauer, *Phys. Rev. A*. 2007, **76**, 033201.
65. M. Kundu, D. Bauer, *Phys. Rev. Lett.* 2006, **96**, 123401.
66. M. Schultze et al., *Science* 2010, **328**, 1658
67. M. Durach, A. Rusina, M. F. Kling, and M. I. Stockman, *Phys. Rev. Lett.* 2010, **105**, 086803.
68. J. Ullrich, A. Rudenko, and R. Moshhammer, *Annual Review of Physical Chemistry* 2012, **63**, 635.